

STUDY ON THE CORRELATION OF TOUGHNESS WITH CHEMICAL COMPOSITION AND TENSILE TEST RESULTS IN MICROALLOYED API PIPELINE STEELS

H. Pouraliakbar^a, G. Khalaj^{b,*}, M.R. Jandaghi^a, M.J. Khalaj^b

^aDepartment of Advanced Materials, World Tech Scientific Research Center (WT-SRC), Tehran, Iran

^bDepartment of Materials Engineering, Saveh Branch, Islamic Azad University, Saveh, Iran

(Received 25 May 2014; accepted 25 July 2015)

Abstract

In this investigation, an artificial neural network model with feed forward topology and back propagation algorithm was developed to predict the toughness (area underneath of stress-strain curve) of high strength low alloy steels. The inputs of the neural network included the weight percentage of 15 alloying elements and the tensile test results such as yield strength, ultimate tensile strength and elongation. Developing the model, 118 different steels from API X52 to X70 grades were used. The developed model was validated with 26 other steels from the data set that were not used for the model development. Additionally, the model was also employed to predict the toughness of 26 newly tested steels. The predicted values were in very good agreement with the measured ones indicating that the developed model was very accurate and had the great ability for predicting the toughness of pipeline steels.

Keywords: *Artificial neural network; Modeling; Toughness; Tensile test; Microalloyed steel; Chemical composition*

1. Introduction

HSLA steels are low-carbon steels (< 0.2 wt% C) containing up to 1.5 wt% manganese (Mn) to produce solid solution strengthening of the ferrite and small amounts (usually < 0.5 wt%) of other alloying elements such as copper (Cu), titanium (Ti), vanadium (V), niobium (Nb), aluminum (Al), silicon (Si), calcium (Ca) and molybdenum (Mo) to provide strengthening and control sulfide and oxide inclusion sizes and to improve the formability [1, 2]. HSLA steels are also strengthened by special rolling and cooling techniques [3, 4]. The chemical compositions of specific HSLA steels may vary for different product requirements to meet the desired mechanical properties. Typically, this group of steels has a microstructure consisting mainly of ferrite and pearlite with highlighted tensile characteristics. Their yield strength is in the range of 275-550 MPa, while their tensile strength ranges from 379 to 620 MPa. Their high strength is obtained by microalloying, grain refinement, controlling the shape of the inclusions, manganese content, and controlled rolling [5, 6]. In order to prevent failures in pipelines, it is important to have high impact toughness and high strength. This is a big challenge for the HSLA steels since it is difficult to keep both strength and impact toughness

high at the same time. Any increase in strength is usually accompanied by a decrease in toughness.

Due to their high strength and toughness, HSLA steels are used mostly in large welded structures such as trains, bridges, buildings, storage tanks, high pressure vessels, ships and submarines [7, 8]. In recent years, most of the oil and gas transportation pipelines are made of HSLA steel grades such as X65 and X70. They have high yield and toughness which enables using them in high gas pressure pipelines with tight safety margins [9, 10].

Recently, artificial neural networks (ANNs) have been widely used for investigating the correlation between final mechanical properties and the chemical composition and/or processing parameters of different steel types [11-17]. In this paper the effects of chemical compositions (containing 15 variables) and tensile strength parameters on the toughness (area underneath of stress-strain curve) of API pipeline steels were modeled using ANN approach.

2. Material and methods

Tensile test procedure conformed to the requirements of API 5L standard [18]. Flat test samples were cut in hoop orientation parallel to the

* Corresponding author: gh.khalaj@srbiau.ac.ir

direction of maximum stress while base metal specimens had gauge length of 50 mm. A 600 kN Zwick tensile testing machine with hydraulic clamps and computer data logger was used for testing in this research. All tensile experiments were conducted at room temperature under displacement control with ram displacement speed of 0.05 mm s^{-1} . In each test, the applied load and specimen elongation were measured. An extensometer with 50.8 mm gauge length was used to monitor specimen axial strains. The computer software gave yield strength (YS) at 0.5% total elongation according to API 5L, ultimate tensile strength (UTS), and specimen elongation percentage in 50.8 mm gauge length at fracture point for each test.

In total, 170 tensile data were obtained from tensile testing. The YS, UTS and specimen elongation were obtained from base metal experiments according to tested standard recommendations [19]. Table 1 listed the statistical parameters of the data used for modeling procedure.

Alloy compositions (containing C, Si, Mn, P, S, Cu, Ni, Cr, Mo, Ti, V, Nb, Ca, Al, B elements) and tensile test results (YS, UTS, elongation) were the 18 independent input parameters and toughness (the area underneath of stress-strain curve) was the output parameter. 170 datasets from API X52, X60, X65 and X70 steels were randomly divided into 118 and 26 groups and were used for training, validating and testing the results, respectively.

3. Results and discussion

3.1. Statistical considerations of tensile data

Tensile test data, like other statistical quantities, can be described by their mean, standard deviation and distribution type. Meanwhile, the probability density is defined as the number of occurrences divided by the total sample number. If the tensile test data are given in the form of Gaussian or normal distribution, the probability density function (PDF), for each set, is calculated as follows [20]:

$$f(x) = \frac{1}{SD\sqrt{2\pi}} \exp\left[-\frac{1}{2}\left(\frac{x-\text{mean}}{SD}\right)^2\right] \quad (1)$$

where SD is the standard deviation of test data in each set, x is the measured strength (in MPa), and mean is the average strength (in MPa) in each dataset.

Table 2 listed all the 104 test results from tension examinations together with target values given in API 5L for X70 steel that are used in modeling. As can be seen, the material's tensile properties fulfilled the API specifications ($485 < \text{YS} < 635$ and $570 < \text{UTS} < 760$ MPa) for API X70 steel grade.

Fig. 1 demonstrates the frequency distribution of YS and UTS values for base metals. Accordingly, the

most occurrences of YS (37 %) and UTS (38 %) were associated with strength ranges 520-540 MPa and 620-640 MPa, respectively. These were close to the obtained YS and UTS average values of 521 (SD = ± 22) MPa and 619 (SD = ± 18) MPa for API X70, respectively.

In Fig. 2 and Fig. 3, the cumulative probability and PDF of material's strength are demonstrated, respectively.

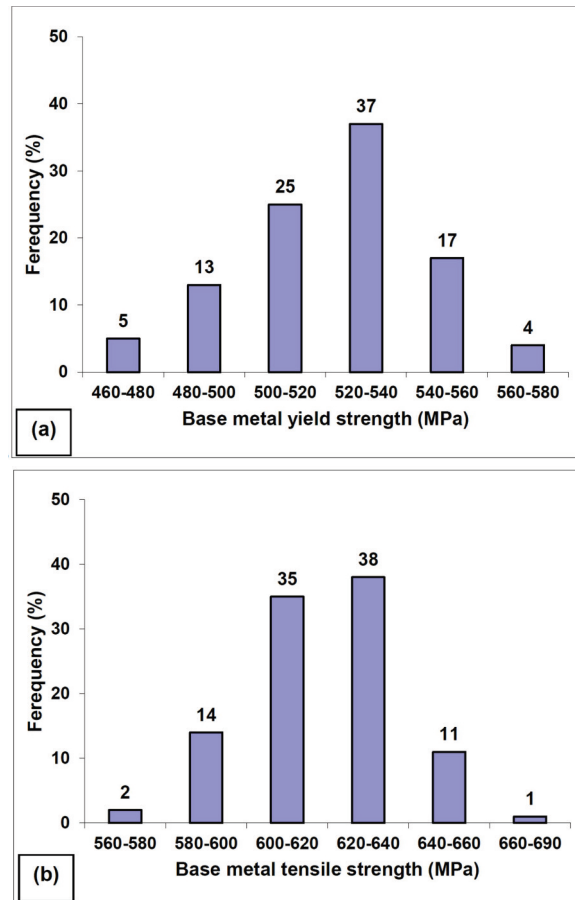


Figure 1. Repetition frequency of (a) yield strength and (b) ultimate tensile strength in API X70 steel

3.2. Correlation between yield and tensile strength

Fig. 4 demonstrates a linear relationship between tensile and yield strength of API steels with relatively low scatter ($R^2 = 0.92$). It shows rising trend in tensile strength with an increase in material's YS, as expected. Fig. 5 shows the variation of toughness versus Charpy impact energy at $-10 \text{ }^\circ\text{C}$ (J) for API X52, X60, X65 and X70 steel grades. The graph shows a linear relationship of area underneath of stress-strain curve with impact toughness with low correlation coefficient ($R^2 = 0.75$) indicating relative scattering. As can be seen from the plot, the scatter

Table 1. Statistical parameters of input and target data

| Statistical parameter | Chemical composition (wt%) | | | | | | | | | | | | | | |
|-----------------------|----------------------------|-----------|----------|----------|----------|----------|----------|----------|----------|----------|----------|----------|----------|----------|----------|
| | C | Si | Mn | P | S | Cu | Ni | Cr | Mo | Ti | V | Nb | Ca | Al | B |
| Minimum | 0.02594 | 0.14068 | 0.92814 | 0.00567 | 0.00008 | 0.01147 | 0.01236 | 0.01174 | 0.0001 | 0.00161 | 0.00001 | 0.00033 | 0.00033 | 0.02117 | 0.00001 |
| Maximum | 0.16161 | 0.28466 | 1.48408 | 0.01777 | 0.00526 | 0.04597 | 0.19698 | 0.14107 | 0.12388 | 0.03606 | 0.00001 | 0.04195 | 0.00406 | 0.04896 | 0.00039 |
| Average | 0.078966 | 0.196312 | 1.362982 | 0.009874 | 0.001454 | 0.019807 | 0.105665 | 0.08742 | 0.079378 | 0.010938 | 0.00001 | 0.032759 | 0.001527 | 0.033782 | 0.000133 |
| Standard deviation | 0.018532 | 0.031498 | 0.150217 | 0.002352 | 0.000861 | 0.008589 | 0.065271 | 0.048841 | 0.050261 | 0.006346 | 2.21E-20 | 0.008521 | 0.000556 | 0.003946 | 5.55E-05 |
| Skewness | 1.311188 | 1.223.797 | -1.60413 | 0.914372 | 2.152257 | 1.346321 | -0.36942 | -0.45433 | -0.92393 | 1.157939 | -1.00892 | -1.9138 | 2.266478 | -0.15077 | 2.294315 |
| Kurtosis | 6.497443 | 0.518024 | 1.443024 | 0.70609 | 5.952727 | 1.064898 | -168769 | -1.74196 | -1.08382 | 2.914537 | -2.02395 | 3.81659 | 7.247511 | 1.451936 | 7.380276 |

Table 1. continued

| Statistical parameter | Mechanical properties | | | |
|-----------------------|-----------------------|-----------|----------------|---|
| | Yield at 0.5 (MPa) | UTS (MPa) | Elongation (%) | Toughness (J.m ⁻³ .10 ⁴) |
| Minimum | 314.74 | 415.41 | 30 | 323 |
| Maximum | 570.78 | 684.79 | 43 | 786.6 |
| Average | 493.4892 | 590.6762 | 35.42353 | 642.5911 |
| Standard deviation | 46.46229 | 46.67979 | 2.283859 | 190.7949 |
| Skewness | -1.17966 | -1.26752 | 0.51924 | -0.8454 |
| Kurtosis | 2.445306 | 1.919458 | 0.671398 | -1.17095 |

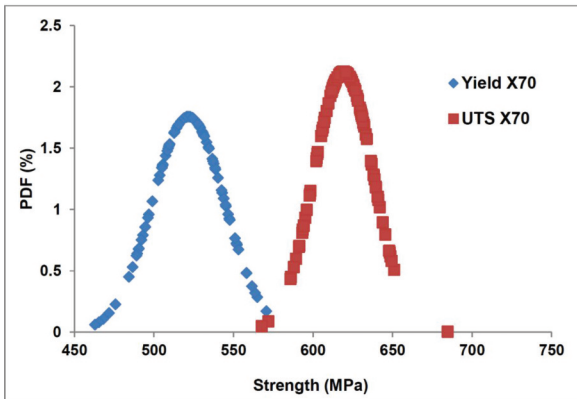


Figure 2. Cumulative probability of strength in API X70 steel grade

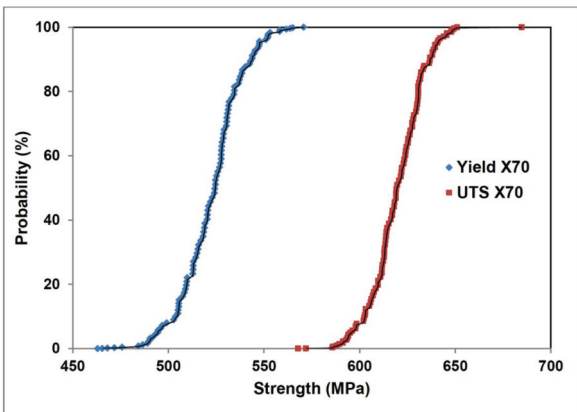


Figure 3. Probability density function of strength in API X70 steel grade

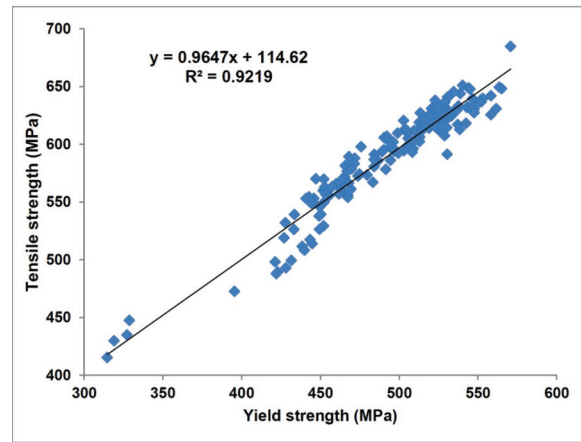
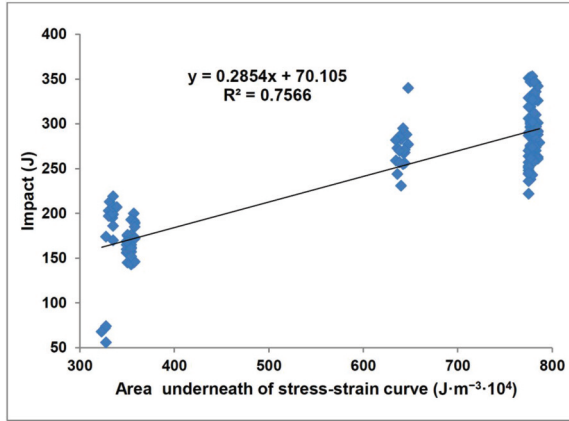


Figure 4. Linear correlation between tensile and yield strength in API X52, X60, X65, and X70 steel grades

in the measured data made it difficult to derive a linear correlation, as is common for steel specimens, between material's area underneath of stress-strain curve and Charpy impact energy. The Charpy impact data were in the range of 56-353 J with an average value of 253 J (all of which conformed with API 5L). On the other hand, area underneath of stress-strain curve fell in the range of 323-786 MPa with an average value of 642 MPa (all of which conformed to API 5L). However, the Charpy impact data for pipe base metals had different values even for the same area underneath of stress-strain curve level. The probable reason for this inconsistency is that tensile test measurement was carried out on full-thickness flat strip specimens in hoop direction. The thick tensile specimen could accurately capture the average tensile strength of the bulk material. However, Charpy impact test measurement was conducted on standard specimen (10×10×55 mm from the same pipe), cut transverse to the rolling axis in accordance to API standard from an area free of defects. Moreover, Charpy values for each pipe are the algebraic average of three discrete measurements.

Table 2. Tensile data of API X70 pipes examined on flat strip

| Property | Minimum | Maximum | Mean | PDF (%) | Standard deviation |
|-----------------------------------|---------|---------|------|---------|--------------------|
| Base metal yield strength (MPa) | 463 | 570 | 521 | 1.7 | 22 |
| Target (MPa) | 485 | 635 | – | – | – |
| Base metal tensile strength (MPa) | 568 | 685 | 619 | 2.1 | 18 |
| Target (MPa) | 570 | 760 | – | – | – |

**Figure 5.** Plot of Charpy impact energy at -10 °C (J) vs. toughness in API X52, X60, X65 and X70 steel grades

3.3 Neural network training and testing

Levenberg-Marquardt feed-forward back-propagation algorithms with sigmoid tangent function were used for training the input data. For ANN modelling, several trials were performed until a high performance model with the highest coefficient of determination (R^2) and the lowest errors was obtained in training, validating and testing phases. Schematic illustration of the network used in this study for ANN model is illustrated in Fig. 6. The input, output and hidden layers were completely interconnected by weights.

The performance of the models was assessed based on R^2 , mean absolute error (MAE), root mean square error (RMSE), relative absolute error (RAE), root relative square error (RRSE) and mean absolute percentage error (MAPE) according to the following equations:

$$R^2 = 1 - \left(\frac{\sum_i (t_i - o_i)^2}{\sum_i (o_i)^2} \right) \quad (2)$$

$$MAE = \frac{1}{n} \sum_i |t_i - o_i| \quad (3)$$

$$RMSE = \sqrt{\frac{1}{n} \sum_i (t_i - o_i)^2} \quad (4)$$

$$RAE = \frac{\sum_i |t_i - o_i|}{\sum_i \left| t_i - \frac{1}{n} \sum_i t_i \right|} \quad (5)$$

$$RRSE = \sqrt{\frac{\sum_i (t_i - o_i)^2}{\sum_i \left(t_i - \frac{1}{n} \sum_i t_i \right)^2}} \quad (6)$$

$$MAPE = \frac{100}{n} \sum_i \frac{|t_i - o_i|}{t_i} \quad (7)$$

where t_i is the target parameter, o_i is the output parameter and n is the number of datasets. The reliability and robustness of a neural network depend on many parameters including “learning constants”, “activation function” and “random distribution of the weights in the initiation of training process” and “the number of nodes in the hidden layer”. The small number of nodes in the hidden layer leads to low fitting and the high number causes over fitting. Some neural networks with 12 to 36 nodes in the hidden layer were trained and the MAPE value for training and testing datasets of these networks was calculated. It was determined that the network with 20 nodes in the first hidden layer and 12 nodes in the second hidden layer had the minimum MRE value for the testing data. The increase in the number of these nodes did not improve the network results for training data. So, the network structure in the present work was 18-20-12-1.

Fig. 7 illustrates the results of training, testing and validating phases for ANN model. From figures, the proposed model is capable of predicting area underneath of stress-strain curve. The model in all phases has the R^2 values more than 99 %. Therefore, it is suggested that ANN model can be suitably used for prediction of displacement. Generally, an ANN

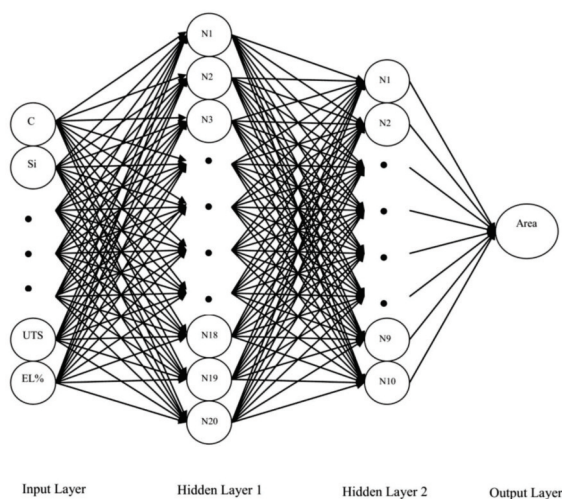


Figure 6. Structure of the ANN model

model is of high performance when it has the highest R^2 and the lowest errors. However in complicated models, when R^2 in training phase increases, values of testing and validating phases decrease. This is called over fitting which must be avoided in artificial intelligence modeling. Here, the difference between R^2 in training, testing and validating phases are not high and therefore one may conclude that over fitting has not been occurred in the proposed ANN model.

Table 3 illustrates the different types of errors for ANN model. Minimum values of MAE, RMSE, RRSE, RAE and MAPE were in training phase and maximum values were in testing phases, listed as expected.

Fig. 8 exemplifies that by increasing sum of errors, R^2 values were decreased. Another performance evaluator can be represented in accordance with Fig.9. Accordingly, errors (differences between output and target values, i.e. $(t_i - o_i)$) and percent errors are plotted versus percent frequency.

Figures show that ANN model had the high performance. 72% of total numbers of datasets had errors between -5 and +5, and 85% of total numbers of datasets had error percents less than 1 %. Fig.10 illustrates that by

Table 3. Errors of ANN model

| | Training | Validating | Testing |
|-------|----------|------------|----------|
| MAE | 3.380508 | 3.769231 | 6.573077 |
| RMSE | 3.908953 | 4.70319 | 7.845013 |
| RAE | 0.019088 | 0.031085 | 0.039356 |
| RRSE | 0.019988 | 0.030514 | 0.041555 |
| MAPE | 0.532805 | 0.559455 | 1.053493 |
| R^2 | 0.999964 | 0.999956 | 0.999867 |

increasing the target values, output errors' trend changed from positive values to negative ones.

4. Conclusion

Variations of mechanical properties in the base metal of 104 test microalloyed steel pipes were measured and compared to API 5L standard

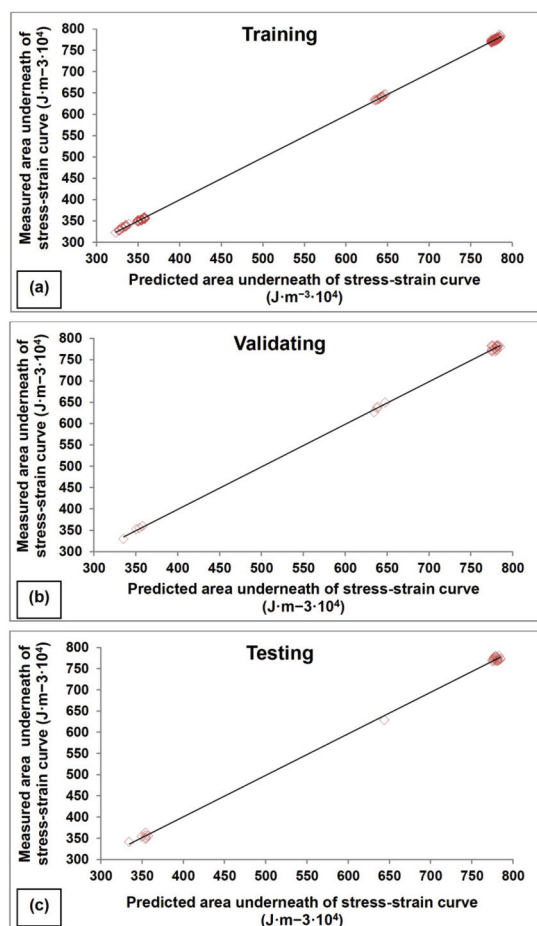


Figure 7. Results from ANN model in (a) training; (b) validating and (c) testing phases

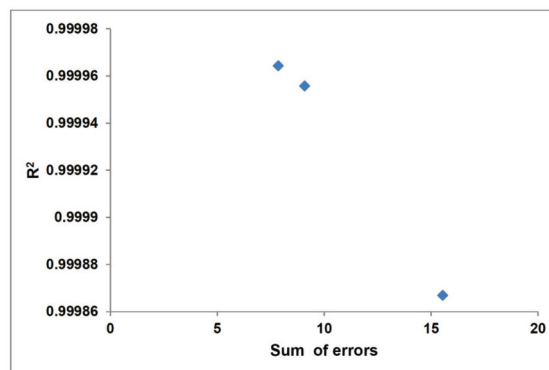


Figure 8. R^2 vs. sum of errors (MAE + RMSE + RAE + RRSE + MAPE) in ANN model

specification to qualify the steel performance under design criteria. Standard full-thickness flat strips were used for tensile testing from which yield strength, tensile strength and maximum elongation were determined for each pipe. The minimum, maximum, mean and standard deviations of measured mechanical properties were calculated for statistical variation and difference of mean value in each pipe. All test data were described by probability density function while the

zones with the largest variance were determined. In this study, ANN model with two hidden layer were developed to predict toughness in terms of area underneath the stress-strain curve of pipeline. Evaluation of the proposed model showed that ANN model was capable of predicting toughness values which were very close to the simulated results. A comprehensive evaluation by means of R^2 , different errors and values of training, testing and validating phases was conducted. As a result, proposed model was capable of predicting area underneath the stress-strain curve with accuracy more than 99 %.

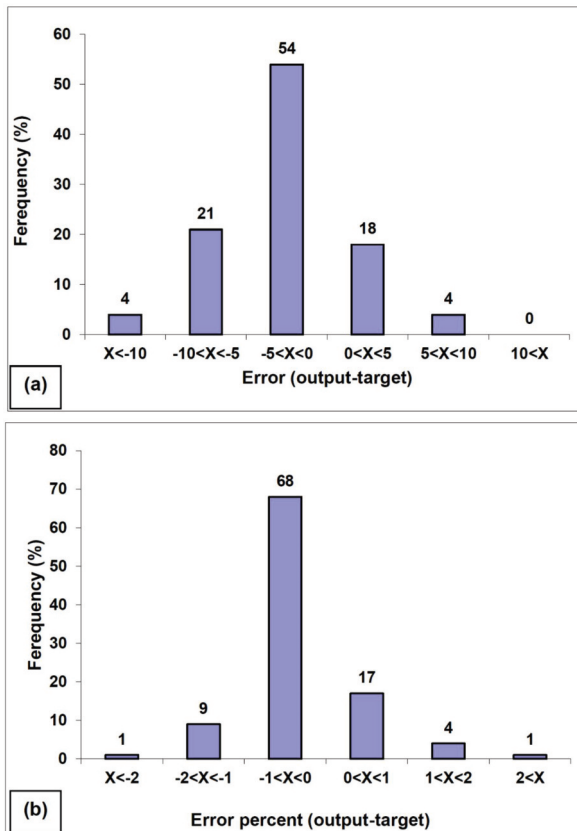


Figure 9. Repetition frequency of (a) error and (b) error percent

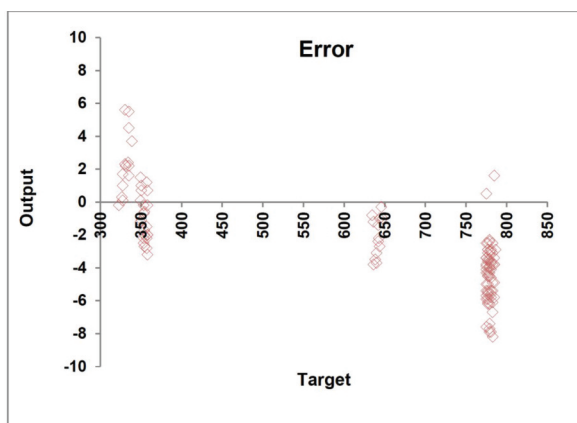


Figure 10. Variation of output vs. target error values

References

- [1] Y. Weng, H. Dong, Y. Gan, *Advanced Steels: The Recent Scenario in Steel Science and Technology*, Springer Science & Business Media, Berlin, 2011.
- [2] H. Bhadeshia, R. Honeycombe, *Steels: Microstructure and Properties: Microstructure and Properties*, Butterworth-Heinemann, 2011.
- [3] B. Verlinden, J. Driver, I. Samajdar, R.D. Doherty, *Thermo-mechanical processing of metallic materials*, Elsevier Ltd, 2007.
- [4] A. Haldar, S. Suwas, D. Bhattacharjee, *Microstructure and Texture in Steels: and Other Materials*, Springer Science & Business Media, London, 2009.
- [5] T. Gladman, *The physical metallurgy of microalloyed steels*, The Institute of Materials, University Press, Cambridge, 1997.
- [6] J.R. Davis (Editor), *High-Strength Low-Alloy Steels, Alloying: Understanding the Basics*, ASM International, Metals Park, Ohio, 2001.
- [7] M.C. Zhao, K. Yang, Y. Shan, *Mater. Sci. Eng. A* 335 (2002) 14-20.
- [8] I.H.G. Hillenbrand, I.M. Graf, I.C. Kalwa, *Development and production of high strength pipeline steels*, Proceedings of the Conference Niobium 2001, Orlando, FL, USA, 2001.
- [9] I.S. Bott, L.F.G. Souza, J.C.G. Teixeira, P.R. Rios, *Metallurgical and Materials Transactions A* 36 (2005) 443-454.
- [10] A. Takahashi, M. Iino, *ISIJ Int.* 36 (2) (1996) 235-240.
- [11] G. Khalaj, H. Yoozbashizadeh, A. Khodabandeh, A. Nazari, *Neural Comput. Appl.* 22 (2013) 879-888.
- [12] S. Hosseini, A. Zarei-Hanzaki, M. Yazdan Panah, S. Yue, *Mater. Sci. Eng. A* 374 (2004) 122-128.
- [13] G. Khalaj, A. Nazari, H. Pouraliakbar, *Neural Network World* 23 (2013) 117-130.
- [14] G. Khalaj, T. Azimzadegan, M. Khoeini, M. Etaat, *Neural Comput. Appl.* 23 (2013) 2301-2308.
- [15] G. Khalaj, M. Khoeini, M. Khakian-Qomi, *Neural Comput. Appl.* 23 (2013) 769-777.
- [16] M.J. Faizabadi, G. Khalaj, H. Pouraliakbar, M.R. Jandaghi, *Neural Comput. Appl.* 25 (2014) 1993-1999.
- [17] N. Narimani, B. Zarei, H. Pouraliakbar, G. Khalaj, *Measurement* 62 (2015) 97-107.
- [18] *API Specifications 5L, Specifications for Line Pipe*, 44th ed., American Petroleum Institute, 2007.
- [19] *Iranian Petroleum Standards (IPS), Material and Equipment Standard for Line Pipe*, Second ed., 2004.
- [20] J.K. Nisbett, R.G. Budynas, *Shigley's Mechanical Engineering Design*, 8th ed., McGraw-Hill Companies, 2006.